Check for updates

Biosorption behavior and mechanism of cadmium from aqueous solutions by *Synechocystis* sp. PCC6803†

Li Shen, [ID] [abc] Ran Chen,[a] Junjun Wang,[d] Ling Fan,[a] Linlin Cui,[a] Yejuan Zhang,[a] Jinju Cheng,[a] Xueling Wu,[ab] Jiaokun Li[abd] and Weimin Zeng [ID] *[ab]

Cyanobacteria are promising adsorbents that are widely used for heavy metal removal in aqueous solutions. However, the underlying adsorption mechanism of *Synechocystis* sp. PCC6803 is currently unclear. In this study, the adsorption behavior and mechanism of cadmium (Cd^{2+}) were investigated. Batch biosorption experiments showed that the optimal adsorption conditions were pH 7.0, 30 °C, 15 min, and an initial ion concentration of 4.0 mg L^{-1}. The adsorption process fitted well with the pseudo-second order kinetic model, mainly based on chemisorption. Complexation of Cd^{2+} with carboxyl, hydroxyl, carbonyl, and amido groups was demonstrated by Fourier-transform infrared spectroscopy (FTIR), Raman spectroscopy and X-ray photoelectron spectroscopy (XPS) analyses. Scanning electron microscopy (SEM), transmission electron microscopy (TEM), and energy-dispersive X-ray spectrometry (EDX) analyses confirmed the presence of Cd^{2+} on the cyanobacterial cell surface and intracellularly. Cd^{2+} could lead to reactive oxygen species (ROS) accumulation and photosynthesis inhibition in cyanobacterial cells, and glutathione (GSH) played an important role in alleviating Cd^{2+} toxicity. Analyses of three-dimensional fluorescence spectroscopy (3D-EEM) and high performance anion exchange chromatography-pulsed amperometric detection (HPAEC-PAD) revealed the changes of the composition and content of EPS after Cd^{2+} adsorption, respectively. Real-time quantitative polymerase chain reaction (RT-qPCR) revealed the potential molecular regulatory mechanisms involved in Cd^{2+} biosorption. These results revealed the adsorption mechanism of Cd^{2+} by *Synechocystis* sp. PCC6803 and provided theoretical guidance for insight into the biosorption mechanisms of heavy metals by other strains.

1. Introduction

Environmental pollution caused by heavy metals has become a global issue of great concern due to mineral extraction, water treatment, metal molding, metal coating, and the battery industry.[1] Heavy metals are non-biodegradable and highly toxic to the environment and can be enriched through the food chain, posing a serious threat to human health and the ecosystem. Cd^{2+} is non-essential element and its compounds are considered to be the most toxic substances in the environment. Heavy metals can cause oxidative stress by excessive accumulation of ROS.[2,3] In addition, prolonged exposure to Cd^{2+} can result in dysfunction of the

kidneys, liver, and central nervous system.[4] Hence, the removal of heavy metals from aqueous environments is necessary for both public and environmental health.

Traditional methods for removing heavy metals from water environments include chemical precipitation, ion exchange, and membrane filtration.[5] However, most of these methods have a series of disadvantages, such as high operating costs, ineffectiveness, and sludge generation. In recent decades, biosorption has been widely investigated and considered a promising alternative to conventional processes because of its low cost, material regeneration, environmental friendliness, and high performance.[6] Various types of biological adsorbents, including fungi, bacteria, yeast, and algae, have been widely applied to remove heavy metals from aqueous solutions.[1,5,7]

Cyanobacteria are photoautotrophic, prokaryotic, and unicellular microorganisms that usually live in aqueous environments. They are promising biosorbents owing to their high photosynthetic efficiency, simple structure, large surface area, and high uptake capacity.[5,8] In addition, cyanobacteria can produce EPS in response to heavy metal toxicity. EPS are heterogeneous macromolecules composed of polysaccharides, proteins, lipids, and nucleic acids.[9] EPS have multiple

[a]*School of Minerals Processing and Bioengineering, Central South University, Changsha 410083, China. E-mail: zengweimin1024@126.com; Fax: +86-731-88879815; Tel: +86-731-88877472*

[b]*Key Laboratory of Biometallurgy, Ministry of Education, Changsha 410083, China*

[c]*State Key Laboratory of Complex Nonferrous Metal Resources Clean Utilization, Kunming 650093, China*

[d]*School of Metallurgy and Environment, Central South University, Changsha 410083, China*

† Electronic supplementary information (ESI) available. See DOI: 10.1039/d1ra02366g

functional groups, including hydroxyl, carboxylic acid, amide, and carbonyl groups, which are likely responsible for the high binding affinity with metal ions.[10] EPS can prevent heavy metal ions from entering the cells of microorganisms by electrostatic attraction, complexation, ion exchange, surface precipitation, and other interaction types. In addition, cyanobacteria have developed antioxidant system mechanisms to alleviate oxidative damage caused by heavy metal stress, including enzymatic antioxidants such as superoxide dismutase, catalase, and peroxidase, and non-enzymatic antioxidants such as GSH, ascorbate, and phenolic substances.[11] These defense strategies help cyanobacteria reduce oxidative impairment and improve heavy metal tolerance.

Biosorption usually includes passive adsorption on the cell surface and active adsorption within cells (bioaccumulation), passive biosorption is a rapid adsorption process independent of energy. The process of active adsorption is much slower and metabolism-dependent.[5,12] However, most adsorption mechanisms are currently unclear. In addition, most related studies have focused on the adsorption behavior and removal efficiency of metal ions, while tolerance and biosorption mechanisms by *Synechocystis* sp. PCC6803 have not been widely investigated. Hence, this study laid the foundation for in-depth understanding of the adsorption mechanism of *Synechocystis* sp. PCC6803 or other species in response to heavy metals. In this study, the factors affecting biosorption conditions, such as pH, temperature, contact time, and initial metal concentration were investigated. Adsorption kinetics were employed to explore the adsorption behavior. FTIR, RS, XPS, SEM, and TEM analyses were performed to explore the adsorption mechanism between *Synechocystis* sp. PCC6803 and cadmium (Cd^{2+}) ions. Moreover, RT-qPCR were used to explore the transcriptional response to Cd^{2+} stress, which may assist with understanding the molecular mechanisms underlying the Cd^{2+} resistance and adsorption.

2. Materials and methods

2.1 Cultivation of *Synechocystis* sp. PCC6803 and effect of Cd^{2+} stress on cyanobacteria growth

The cyanobacteria strain *Synechocystis* sp. PCC6803 was originally purchased from the Freshwater Algae Culture Collection at the Institute of Hydrobiology of China (FACHB). *Synechocystis* sp. PCC6803 cells were grown in conical flasks containing BG-11 medium and placed in a light incubator for static cultivation. Cultivation was performed under a light/dark cycle of 12/12 h with a moderate light intensity of 2000 lx at 25 °C.[13] Before the experiment, all instruments and medium were sterilized at 121 °C for 20 min to prevent contamination. During the cultivation period, all flasks were shaken by hand twice daily to avoid agglomeration. In addition, the position of the flasks was changed randomly to reduce the influence of light intensity, as per a previous study.[14]

The Cd^{2+} solution was prepared by adding $CdCl_2$ to sterile water to form 1 g L^{-1} mother liquor. Cd^{2+} solutions were sterilized by filtering them with a 0.22 μm pore size filter.[15] Cd^{2+} solution was separately added to a 250 mL conical flask with 100 mL of culture medium to obtain the final concentrations of 0, 0.25, 0.5, 0.75, 1.0, 1.25, 1.5, and 2.0 mg L^{-1}, and the medium without Cd^{2+} was defined as the control. Cyanobacteria growth

was determined by measurting the optical density at 730 nm (OD730) under different Cd^{2+} concentrations. The experiments were performed in triplicate. Finally, referred to the chemical-alga growth inhibition test and calculated the 12 day minimal inhibitory concentration (MIC) for *Synechocystis* sp. PCC6803.

2.2 Determination of non-enzymatic features

After 12 days of cultivation (cells were in the logarithmic phase), the cyanobacteria cells were exposed to Cd^{2+} for 96 h. Cells were harvested by centrifugation and washed twice with 0.05 M phosphate-buffered saline (pH 7.0) for the following physio-biochemical analysis. Under 1.0 mg L^{-1} of Cd^{2+} stress, the contents of chlorophyll and carotenoid, malondialdehyde (MDA), GSH, and ROS were quantified after exposure to Cd^{2+} for 0 h, 15 min, 24, 48, 72, and 96 h using assay kits (Beijing Solarbio Science &Technology, Beijing; Suzhou Comin Biotechnology, Suzhou, China) according to the manufacturer's instructions. The absorbance of the samples was measured using an ultraviolet spectrophotometer (L5S, Shanghai, China). All sample tests were performed in three biological replicates.

2.3 EPS extraction, 3D-EEM, and HPAEC-PAD analyses

When cyanobacteria growth reached the logarithmic phase based on our previous study, Cd^{2+} was added to the medium, and medium without Cd^{2+} served as the control. Each treatment was performed in triplicate. The sampling times were 0 h, 15 min, 24, 48, 72, and 96 h. EPS extraction was performed using the methods of Xu *et al.*,[16] all EPS fractions were filtered with 0.45-um membrane filters to remove cell precipitations and other suspended particles.[13] The EPS supernatant was stored at −20 °C for further characterization.

The 3D-EEM spectra of the EPS solution were recorded using a fluorescence spectrophotometer (F-7000, Hitachi, Japan). The 3D-EEM spectra were collected at 10 nm increments over an excitation range of 200–450 nm with an emission range of 250–550 nm every 5 nm. The excitation and emission slits were set to 2.5 nm of band-pass and the scan speed was set at 1200 nm min^{-1}.[17,18] Finally, 3D-EEM data were processed using the Origin 8.0. The measurements were taken in triplicate and the mean values were used for model fitting.

The HPAEC-PAD method was mainly used to analyze the exopolysaccharide components. After EPS extraction, 5 mL of 2 M trifluoroacetic acid was added to the EPS and hydrolyzed at 120 °C for 3 h. Then, the acid hydrolysis solution was accurately absorbed and transferred to a tube for nitrogen blow-drying. Next, 1 mL of water was added, and the solution was vortexed by centrifugation at 12 000 rpm for 5 min. Finally, remained the supernatant for HPAEC-PAD (ICS5000+ DC, Thermo) analysis.

2.4 Batch biosorption experiments

The effects of pH, temperature, initial Cd^{2+} concentration, and contact time on biosorption efficiency were evaluated.[19] The effect of pH was determined at 1.0 mg L^{-1} Cd^{2+} and a fixed speed of 180 rpm using solutions with different initial pH values from 2.0 to 8.0 for 3 h. The initial pH was adjusted by adding HCl and NaOH solutions. The effect of temperature was determined at 1.0 mg L^{-1} Cd^{2+} and pH 7.0, with temperatures

ranging from 20 °C to 40 °C for 3 h of contact time. The initial Cd^{2+} from 0 to 30 mg L^{-1} was performed at optimum conditions of pH 7.0 and 30 °C. The effect of contact time was set to 0 h, 5 min, 10 min, 15 min, 30 min, 1 h and 3 h at 1.0 mg L^{-1} Cd^{2+} with optimum conditions of pH 7.0 and 30 °C. After biosorption, the cell suspensions were centrifuged at 8000 rpm for 5 min and the supernatant was collected for Cd^{2+} concentration determination by inductively coupled plasma-optical emission spectrometry (ICP-OES; Optima 5300 DV, PerkinElmer, USA). The biosorption efficiency of Cd^{2+} was calculated using the following formula:[12]

$$\text{Adsorption efficiency (\%)} = (C_0 - C_t)/C_0 \times 100\%$$

where C_0 is the initial Cd^{2+} concentration and C_t is the Cd^{2+} concentration after adsorption at contact time t.

2.5 Zeta potential measurements

The zero-point charge (pH_{pzc}) was determined by mixing 0.01 g cyanobacteria cells with 0.01 M KCl solution (20 mL), and the pH was adjusted to 1–6 using NaOH or HCl solutions.[20] After filtering the adsorbents, the final pH of the solution was determined using a zeta potential analyzer (Zetasizer Nano ZS90, Malvern).

2.6 Adsorption kinetics and desorption experiments

The kinetics of adsorption is needed to determine the adsorption velocity.[4] Two kinetic models including pseudo-first and -second order kinetic models, were tested to fit the kinetics experimental data. The pseudo-first and -second order kinetic models and formulas are as follows:[21]

$$\ln(q_e - q_t) = \ln q_e - k_1 t$$

$$\frac{t}{q_t} = \frac{1}{k_2 q_e^2} + \frac{t}{q_e}$$

where t is the adsorption time (min), q_t and q_e correspond to the adsorption amount of metal ions (mg g^{-1}) at time t and adsorption equilibrium, and k_1 (min^{-1}) and k_2 (g mg^{-1} min^{-1}) correspond to the pseudo-first and -second order adsorption rate constants, respectively.

The desorption study of Cd^{2+} was performed by treating biosorbents with different desorbents such as 0.1 M EDTA-Na_2, 0.1 M HCl, 0.1 M HNO_3, 0.1 M NaCl, and distilled water.[4,19] The cyanobacteria were first centrifuged at 8000 rpm for 5 min after Cd^{2+} biosorption (pH 7.0, 30 °C, 180 rpm for 3 h) and the supernatants were retained for Cd^{2+} concentration detection. Then, the Cd-adsorbed cyanobacterial precipitations were added to 100 mL of the desorbent in 250 mL conical flasks and shaken at 180 rpm, 30 °C for 3 h. Supernatants were detected as described above by ICP-OES after centrifugation.

2.7 FTIR, Raman spectrum, and XPS analyses

The surface functional groups of *Synechocystis* sp. PCC6803 before and after Cd^{2+} biosorption were evaluated by FTIR spectroscopy (IS5, Thermo Fisher Scientific, USA) and Raman spectroscopy (HORIBA, LabRAM HR Evolution, France). Cyanobacterial precipitations were obtained by centrifugation at 8000 rpm for 5 min, washing twice with deionized water, freeze-drying, and grinding into powder. Samples (30 mg) were pressed with KBr at a ratio of 1 : 100 for FTIR analysis, and 50 mg samples were used for Raman spectrum analysis.

XPS (K-Alpha$^+$, Thermo Fisher Scientific, USA) was used to characterize the oxygen, carbon, and nitrogen valence-electron changes of cyanobacteria before and after Cd^{2+} adsorption. The binding energies were calibrated using the C1s peak with a fixed binding energy of 284.8 eV to compensate for the surface charging effects.[22] Avantage software was used to fit the XPS spectra peaks.

2.8 SEM and TEM-EDX analyses

After 15 min, 24, 48, 72, and 96 h of adsorption with or without 1.0 mg L^{-1} Cd^{2+}, the cyanobacteria cells were used for SEM analysis, cells were fixed with 2.5% glutaraldehyde at 4 °C for 12 h, washed with phosphate buffer (0.05 M, pH 7.0) then dehydrated with 30%, 50%, 70%, 90% and 100% ethanol, finally, freeze-dried samples were coated with gold as reported by Zhang *et al.*[23] The morphology of the cells was observed using scanning electron microscope (MIRA3, Tescan) coupled with EDX analysis (Oxford X-Max 20, UK).

Cyanobacteria cells before and after 1.0 mg L^{-1} Cd^{2+} adsorption were used for TEM analysis, sample preparation was performed according to standard procedures,[24] including cell fixation, dehydration, embedding, ultrathin sectioning, and dyeing. The distribution and morphology of Cd^{2+} on the surface and interior of the cells before and after adsorption were characterized using transmission electron microscopy (H-7650, Hitachi).

2.9 Real-time quantitative PCR

Three genes related to Cd^{2+} adsorption and one gene involved in exopolysaccharides synthesis were selected to calculate expression levels by RT-qPCR. After 15 min, 24, 48, 72, and 96 h of stress with or without 1.0 mg L^{-1} Cd^{2+}, the cyanobacterial suspensions were used to extract total RNA. Total RNA was isolated from the control and stress groups using a plant RNA extraction kit (Tiangen, China). Specific primers for RT-qPCR were designed using Primer Premier 5.0, synthesized by Tsingke Biological Technology (Changsha, China), and the gap1 gene was used as an internal control gene[14] (Table 1). The cDNA synthesized by HiScript II Q RT SuperMix for qPCR containing a gDNA wiper (Vazyme, China) was used as a template for RT-qPCR. RT-qPCR was carried out on a Real-Time PCR Detection Systerm (Gentier 48R, China) with ChamQ Universal SYBR Master Mix (Vazyme, China) according to the manufacturer's instructions. Three experiments were conducted to ensure the accuracy of the results. Relative expression levels were calculated using the $2^{-\Delta\Delta CT}$ method.[25]

2.10 Statistical analysis

All experiments were performed in triplicate, and the data are expressed as the mean ± standard error for each group. Statistical analyses were performed with one-way analysis of variance (ANOVA), and differences were considered significant at p-value <0.05 (SPSS 20.0 version).

Table 1 Primers for the RT-qPCR validation

Gene ID	Annotation name	Forward primer (5′ to 3′)	Reverse primer (5′ to 3′)	Product (bp)
MYO_18125	CusA/CzcA family heavy metal efflux RND transporter	TGGTGACGGAACGGCTAC	TGATGGGAGAAGATACAGGAG	87
MYO_11210	TrkA family potassium uptake protein	CAGGAGGATGCCCTAAAT	TCTGTGGTGCTGATAATGTG	140
MYO_14270	Cadmium-translocating P-type ATPase	CGTGCCTTGGTTCTGTTG	GCCGTGAGGGAGTCTAAAA	140
MYO_05725	Exopolysaccharide biosynthesis protein	TTCTTTCCCTCCCTTCGG	AATGCCTTGGGCCTTGC	167
gap1	Reference gene	GCTACCGCAGTTAAAAGGTA	GTAACTCGTGGCTTTTTCC	106

3. Results and discussion

3.1 Effect of Cd^{2+} stress on the growth of *Synechocystis* sp. PCC6803

To investigate the tolerance of *Synechocystis* sp. PCC6803 to different Cd^{2+} concentrations, the growth performance of cyanobacteria under Cd^{2+} stress was investigated (Fig. 1). The cells grew well in the control group, while the growth curve lagged and the growth rate decreased gradually with increasing Cd^{2+} concentrations during the 12 day culture period. When the Cd^{2+} concentration was 1.0 mg L^{-1}, cell biomass did not increase with the extension of cultivation time. The highest biomass yield (OD730) substantially declined to 0.011 when exposed to 2.0 mg L^{-1} Cd^{2+}, indicating that the inhibitory effect of Cd^{2+} on cyanobacteria growth was dose-dependent. According to chemical-algae growth inhibition tests,[26] the minimal inhibitory concentration (MIC) calculated was 1.18 mg L^{-1} for *Synechocystis* sp. PCC6803. The subsequent experiments were all carried out at 1.0 mg L^{-1} Cd^{2+} concentration.

3.2 Effects of Cd^{2+} stress on the physiology and biochemistry of *Synechocystis* sp. PCC6803

Physiological and biochemical analyses were performed to elucidate the effect of Cd^{2+} stress on cyanobacterial pigments and oxidative stress tolerance, as shown in Fig. 2. In general, the change trends of chlorophyll *a*, chlorophyll *b*, and carotenoid were similar. As the culture time increased, the chlorophyll and
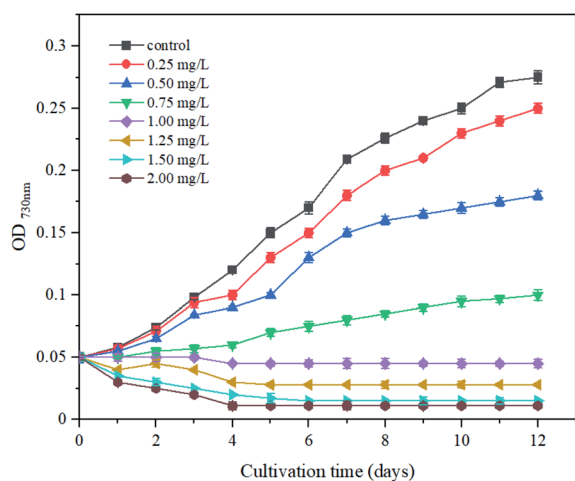

Fig. 1 Effect of different Cd^{2+} concentrations on the growth of *Synechocystis* sp. PCC6803.

carotenoid contents increased in the control, while pigment synthesis was significantly inhibited after Cd^{2+} stress. The chlorophyll *a*, chlorophyll *b*, and chlorophyll *a*+*b* contents of Cd^{2+} stressed samples were 57.28%, 38.13% and 53.79% lower than those in the control at 96 h, respectively (Fig. 2a–c). The carotenoid content in the Cd^{2+} stressed samples decreased by 44.66% compared to that of the control at 96 h (Fig. 2d). Compared with the control, MDA content was the highest at 48 h (64.41% increase) and decreased thereafter (Fig. 2e). GSH content increased gradually and the highest content was observed at 96 h (1.277-fold increase) compared to that of the control (Fig. 2f). H_2O_2 content peaked at 72 h (2.404-fold increase) and then induced (Fig. 2g). The O_2^- content increased gradually and peaked at 96 h (74.34% increase) (Fig. 2h).

Cd^{2+} stress can damage the membrane lipids, proteins and nucleic acids of cyanobacteria cell and disturb the homeostasis of the organism, especially the accumulation of ROS. The increase in H_2O_2 and O_2^- levels may be attributed to the excessive accumulation of ROS.[27] MDA is the end product of lipid peroxidation, and an increase in MDA content could reflect the degree of lipid peroxidation.[28] As a product of sulfur metabolism, GSH is the precursor of phytochelatins, which can chelate with heavy metal ions to reduce Cd^{2+} toxicity.[29] The increase in GSH was responsible for cyanobacteria resisting heavy metal stress. Chlorophyll is closely related to the photosynthetic reaction, and the decrease in chlorophyll content may be due to the distortion of the chlorophyll ultrastructure, inhibition of the synthesis of photosynthetic pigments and enzymes.[30] These results revealed that Cd^{2+} can inhibit cyanobacteria photosynthesis and cause cell oxidative damage, and that GSH played an important role in interacting with Cd^{2+} and relieving metal toxicity. Consequently, the determination results revealed the toxic effects of Cd^{2+} on cyanobacteria and the physiological response mechanism of cyanobacteria in response to Cd^{2+} stress, providing a reference basis for the better application of cyanobacteria in heavy metal wastewater treatment.

3.3 Content changes of EPS before and after Cd^{2+} adsorption

The changes in EPS contents under Cd^{2+} stress are depicted in Fig. 2i and j. Extracellular proteins and exopolysaccharides increased by 13.432% and 29.862% (15 min), 35.105% and 28.013% (24 h), 36.459% and 63.688% (48 h), 64.107% and 69.703% (72 h), and 34.711% and 20.997% (96 h) compared to control group, respectively. Besides, the contents of exopolysaccharides were higher than that of extracellular proteins during the cultivation period, indicating that the EPS of *Synechocystis* sp. PCC6803 was mainly composed of exopolysaccharides, Teng *et al.*[31] also found that the concentrations of
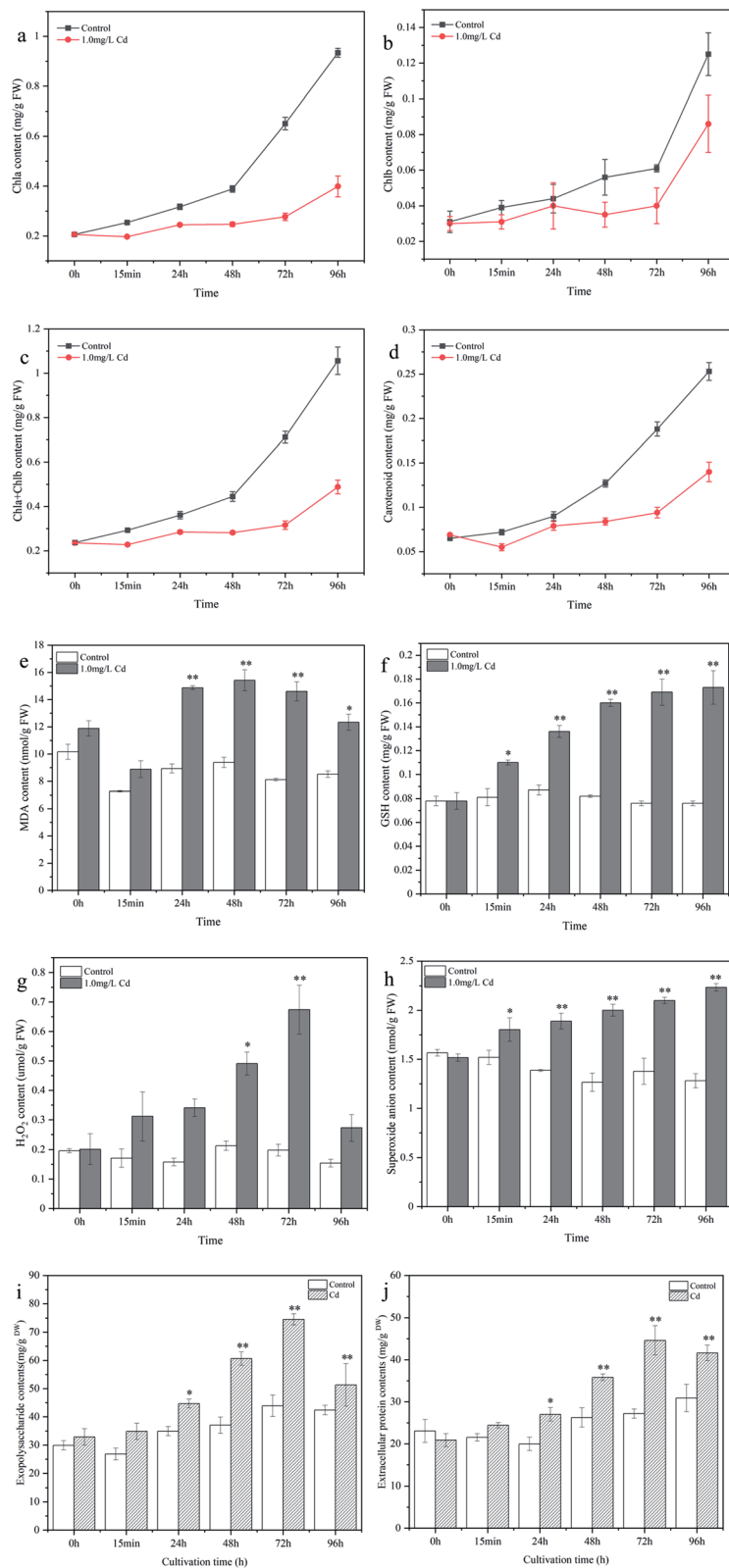
Fig. 2 Changes of chlorophyll *a* (a), chlorophyll *b* (b), chlorophyll *a+b* (c), carotenoid (d), malondialdehyde (e), glutathione (f), hydrogen peroxide (g), superoxide anion (h), exopolysaccharide (i), and extracellular protein (j) contents in *Synechocystis* sp. PCC6803 under Cd^{2+} stress during cultivation time.

protein in EPS were basically less than that of polysaccharides after Pb(II) stress, indicating that polysaccharides was main components of EPS in *Leclercia adecarboxylata*.

Extracellular protein and exopolysaccharide contents showed an obvious increase in the first 72 h, and then decreased slowly at 96 h (still higher than the control) compared to 72 h.

To resist the cellular damage caused by Cd^{2+}, microorganisms tend to secrete EPS as a self-protection strategy against abiotic stress.[31,32] Li *et al.*[33] found that the adsorption of Ni(II) by EPS extracted from AGS and AnGS were 65.77 and 54.18 mg g^{-1}, respectively, suggesting that EPS can make a certain contribution for heavy metal removal from aqueous environment in sludge biosorption process. Ozturk *et al.*[15] also observed a significant and regular increase in EPS production of *Synechocystis* sp. BASO67l by Cr(VI), Cd(II) and Cr(VI) + Cd(II) stress at a concentration of 35 ppm. Extracellular protein and exopolysaccharides were rich in many functional groups, which provide numerous binding sites for metal ions, thus reducing the toxicity to the cells. In addition, as the concentration of free Cd^{2+} in the culture medium decreases, Cd^{2+} stress become weaker, the secretion of EPS is reduced slowly. Therefore, the results obtained in this investigation also showed that the secretion of EPS in *Synechocystis* sp. PCC6803 was regulated by the pressure of heavy metal ions.

3.3.1 3D-EEM analysis.
3D-EEM analysis was applied to characterize the interaction between EPS and heavy metal ions. Exopolysaccharides are non-fluorescent substances, so we focused our analysis on the changes of proteins and humic substances in EPS. As shown in Fig. 3 and Table S1,† four fluorescence peaks were identified at 15 min, 24 h, 48 h and 72 h after exposure to Cd^{2+}, respectively. The fluorescence of peak A ($E_x/E_m = 260–280/450–460$ nm) and B ($E_x/E_m = 350–360/450–460$ nm) was assigned to humic acid-like and humic acid substances.[34] The fluorescence of peak C ($E_x/E_m = 280/340–380$ nm) and D ($E_x/E_m = 220–230/320–340$ nm) was identified as protein-like substances containing tryptophan and tyrosine.[35,36] A new fluorescence peak E ($E_x/E_m = 320/380$ nm) appeared after Cd^{2+} adsorption at 96 h, which was further identified as humic acid-like substances. Compared to the control, the fluorescence intensity of those peaks were enhanced during the cultivation period, indicating that Cd^{2+} induced the secretion of EPS and prevented cell injury by adsorbing Cd^{2+}. The research also showed that the presence of heavy metals can change the content and composition of extracellular proteins.

Previous study have found that fluorescence of humic-like and protein-like fluorophores in *Synechocystis* sp. could be statically quenched by Cu(II), indicating formation of Cu(II)–EPS complexes, confirmed by 3D-EEM.[37] Therefore, it was speculated that biochemical reaction happened between Cd^{2+} and EPS and the increase of extracellular protein was related to heavy metal resistance. In addition, after Cd^{2+} adsorption, various fluorescence peaks have different degrees of red shift (longer wavelengths) or blue shift (shorter wavelengths), which may be related to the increase or reduction of functional groups, such as hydroxyl, carboxyl, carbonyl, and amino groups.[38]

3.3.2 HPAEC-PAD analysis of exopolysaccharides.
The HPAEC-PAD method was used for the accurate quantification of exopolysaccharides.[39] The types and contents of exopolysaccharides before and after Cd^{2+} adsorption are shown in Fig. 4 and Table S2.† The following 11 monosaccharides were isolated: fucose, galactosamine hydrochloride, rhamnose, arabinose, glucosamine hydrochloride, galactose, glucose, xylose, mannose, galacturonic acid, and glucuronic acid. After Cd^{2+} adsorption, the monosaccharide type did not change but the contents of the six monosaccharides increased and those of the remaining five decreased. In addition, the total contents of exopolysaccharides increased from 156.11 to 164.11 mg L^{-1} after adsorption, but the improvement was not significant. The results showed that the content of exopolysaccharides were affected by the presence of heavy metals.
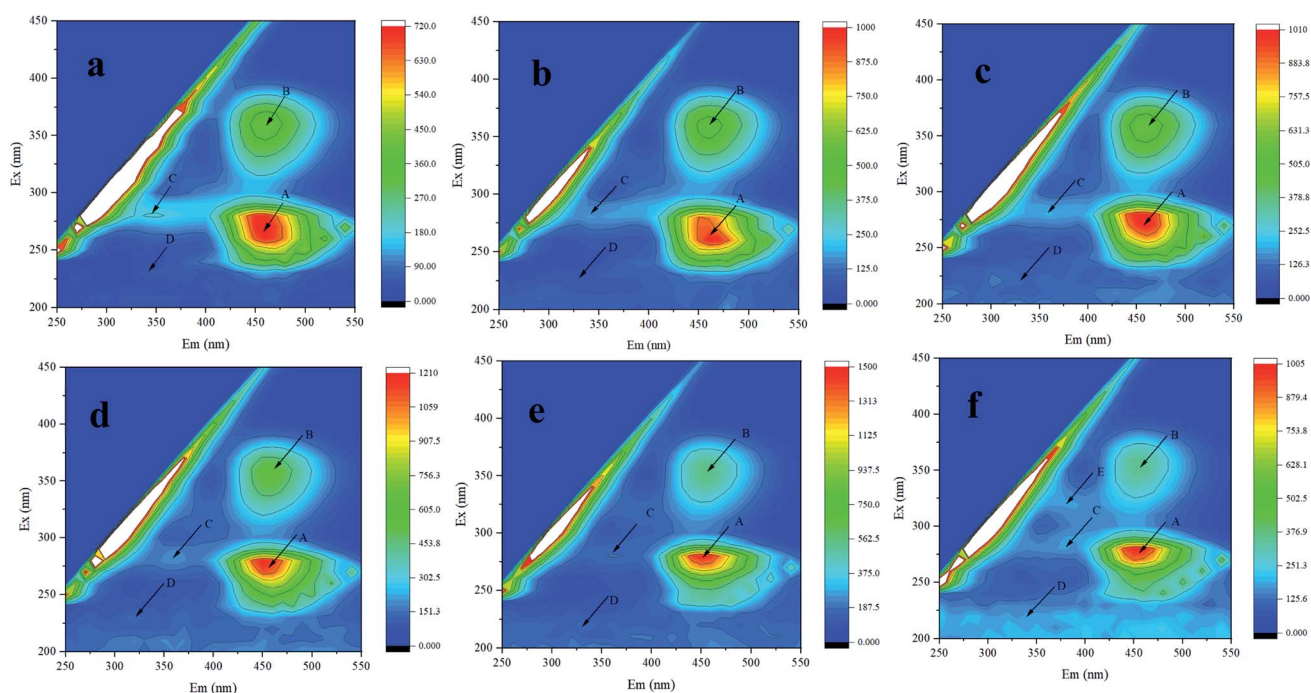

Fig. 3 3D-EEM of *Synechocystis* sp. PCC6803 exposed to Cd^{2+}. (a–f) represent control, 15 min, 24, 48, 72, and 96 h treatment, respectively.
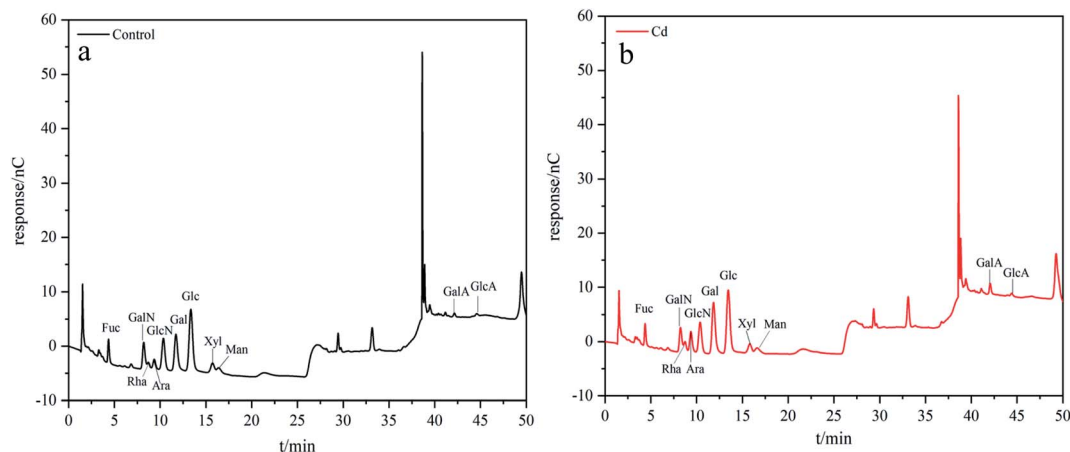
Fig. 4 HPAEC-PAD analysis of exopolysaccharides before (a) and after (b) Cd^{2+} adsorption.

The contents of exopolysaccharides changed after Cd^{2+} adsorption, which could be explained by Cd^{2+} stress potentially effect the expression of exopolysaccharides genes. Therefore, we used RT-qPCR to futher verify the function of exopolysaccharides during Cd^{2+} adsorption process. The expression level of the gene related to exopolysaccharides synthesis was evaluated by RT-qPCR (Fig. 9d). The results of RT-qPCR indicated that the expression level of the exopolysaccharides synthesis gene was up-regulated and most significant at 72 h compared to control, which suggested that the exopolysaccharide gene may participate in regulating the adsorption of heavy metals. Shen et al.[14] also found that the gene expression of exoD, which is found to be related to EPS production, rose 9.31 times after Cd^{2+} exposure for 3 days compared with the initial inoculation in Synechocystis sp. PCC6803. These experimental results demonstrated that exopolysaccharides secreted by cyanobacteria participated in the adsorption and resistance of Cd^{2+} and alleviated toxicity caused by heavy metals.

3.5 Effect of pH, temperature, initial Cd^{2+} concentration, and contact time on adsorption

3.4.1 **Effect of pH.** To investigate the effect of pH on the adsorption efficiency, Cd^{2+} adsorption by cyanobacteria was observed within the pH range of 2.0–8.0. As shown in Fig. S1a,† the adsorption efficiency increased from 3.142% to 64.404% with a pH ranging from 2.0 to 7.0 and optimum biosorption occurred at pH 7.0. Afterwards, a decrease in the Cd^{2+} biosorption efficiency was observed at pH 8.0 with an adsorption efficiency of 62.624%, which can be attributed to surface charge changes of the adsorbents. The pHpzc of the Synechocystis sp. PCC6803 was estimated as 2.5 (Fig. S1a†). When pH <2.5, H^+ competed with Cd^{2+} for adsorption sites on the cell surfaces, thus, a repulsive force exists in the Cd^{2+} and binding sites in the adsorption process.[40] At pH >7.0, metal ions may precipitate from alkaline solutions, leading to a decrease in the adsorption efficiency.[12]

3.4.2 **Effect of temperature.** In this study, the optimum adsorption temperature was determined by setting the range at 20–40 °C. As shown in Fig. S1b,† the adsorption efficiency increased gradually from 20 °C to 30 °C (75.183–77.794% at

2.0 mg L^{-1} Cd^{2+}) and reached a maximum at 30 °C. Afterward, the adsorption efficiency gradually decreased from 30 °C to 40 °C (77.794–74.364% at 2.0 mg L^{-1} Cd^{2+}). Therefore, 30 °C was considered the optimal adsorption temperature. Increasing the temperature enhances the surface activity and kinetic energy of the solute, but excessively high temperatures destroy the binding site on the surface of the adsorbent.[41]

3.4.3 **Effect of initial Cd^{2+}** Effect of initial Cd^{2+} concentration. Fig. S1c† shows the effect of initial Cd^{2+} concentration (0–30 mg L^{-1}) on the adsorption efficiency of cyanobacteria. When the Cd^{2+} concentration increased to 4.0 mg L^{-1}, the adsorption efficiency by cyanobacteria increased to 86.556%. Afterwards, the adsorption efficiency remained stable with the increase of Cd^{2+} concentration, which indicated that the adsorption site reached saturation and lacked sufficient binding sites for metal ion biosorption on the biosorbent surfaces.[42] When the Cd^{2+} concentration >15 mg L^{-1}, the adsorption efficiency decreased sharply. An important factor was that high concentration of Cd^{2+} was toxic to strains and affected strain viability. The toxic effect led to cells death and rose of Cd^{2+} concentration in solution. Similar results have been obtained in previous studies.[12,43]

3.4.4 **Effect of contact time.** The effect of the contact time on the adsorption efficiency of cyanobacteria is shown in Fig. S1d.† Cyanobacteria rapidly reached a high adsorption efficiency of 65.508% in the initial 15 min. Subsequently, the adsorption efficiency reached equilibrium. 15 min was observed to be the optimum adsorption time. Initially, rapid adsorption occurred mainly because the sites on the adsorbent's surface were vacant and the metal ion concentration was high. Subsequently, the adsorption equilibrium was a result of the low metal ion concentrations and saturation of adsorption sites.[40]

Those findings implied that the optimal adsorption conditions for cyanobacteria were pH 7.0, 30 °C, contact time of 15 min, and an initial Cd^{2+} concentration of 4.0 mg L^{-1}. The biosorption of Cd^{2+} by Synechocystis sp. PCC6803 is a complicated process controlled by many environmental variables such as pH, temperature, contact time, and initial Cd^{2+} concentration. Through the adsorption experiment, we can further
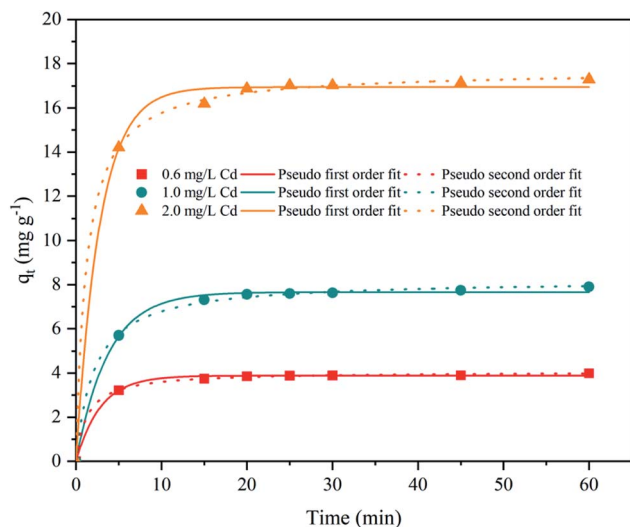
Fig. 5 Adsorption kinetics of Cd^{2+} by *Synechocystis* sp. PCC6803.

understand the effect of heavy metals on the adsorption behavior of *Synechocystis* sp. PCC6803.

3.5 Biosorption kinetics. To investigate the kinetics of Cd^{2+} adsorption on *Synechocystis* sp. PCC6803, pseudo-first and -second order models were used to fit the experimental data of the adsorption kinetics. The adsorption kinetic curves and parameters of the two models are presented in Fig. 5 and Table 2, respectively. Fig. 5 shows that the adsorption capacity increased as Cd^{2+} increased from 0.6 to 2.0 mg L^{-1}. In addition, the adsorption efficiency of Cd^{2+} by cyanobacteria was high in the first 15 min and reached adsorption equilibrium after 25–30 min. As shown in Table 2, the adsorption data fitted well with the pseudo-second order model with R^2 >0.9989, which was higher than that of the pseudo-first order model (R^2 >0.9970). The equilibrium adsorption values (q_e) calculated by the pseudo-second order model were 4.066, 8.213, and 17.712, which were consistent with the theoretical values. Similar results were reported for the Pb^{2+} adsorption process in *Bacillus* strains, and the results showed that the second-order kinetic was superior to the first-order kinetic.[40] Therefore, the adsorption kinetics followed the pseudo-second order model, suggesting that the adsorption mechanism between Cd^{2+} and the adsorbent was mainly chemical adsorption, and chemical reaction was the rate-limiting step in the Cd^{2+} process.[43]

3.6 Desorption of Cd^{2+}. The distribution of the adsorbed Cd^{2+} in the biosorbents was investigated using desorption experiments. Fig. S2† shows the proportion of Cd^{2+} released from the adsorbents after treatment with different desorbents (0.1 M EDTA-Na$_2$, 0.1 M HCl, 0.1 M HNO$_3$, 0.1 M NaCl, and H$_2$O). The results showed that 5.961% Cd^{2+} was desorbed by H$_2$O, and 82.264% and 68.042% Cd^{2+} by HCl and HNO$_3$, respectively. In addition, the desorption efficiency of NaCl and EDTA-Na$_2$ were 18.933% and 65.737%, respectively. It was obviously observed that desorption efficiency: HCl > HNO$_3$ > EDTA-Na$_2$ > NaCl > H$_2$O. Desorption results proved that biosorbent was suitable for reuse after desorbed by HCl.

Cd^{2+} released by NaCl can be regarded as the fraction adsorbed by ion exchange, while the fraction released by EDTA-Na$_2$ was considered to be adsorbed by complexation.[44] Cd^{2+} can also bind weakly by physical trapping, which can be easily desorbed by H$_2$O.[45] For HCl and HNO$_3$, H$^+$ can compete with Cd^{2+} for the binding sites on the adsorbent surface, resulting in the release of Cd^{2+}. Suitable desorbents can make the adsorbents efficiently reused during the metal treatment process. Ghoneim *et al.*[46] also observed that HCl has the highest recovery efficiency for cadmium in *Ulva lactuca*. The desorption experiments suggested that the regeneration of the biosorbents was possible for repeated use with regard to Cd^{2+}.

3.7 FTIR, Raman spectrum, and XPS analyses

3.7.1 FTIR analyses. FTIR analysis was mainly applied to identify the functional groups in the Cd^{2+} adsorption process. The FTIR results before and after Cd^{2+} adsorption are shown in Fig. 6a, and the characteristic peak wavenumbers are listed in Table S3.† Phenomena such as peak shift and peak intensity changes were observed after Cd^{2+} adsorption. The band at 3305.22–3317.16 cm^{-1} was assigned to the stretching vibration of –OH in polysaccharides.[47] The band at 2927.31–2928.54 cm^{-1} was assigned to the stretching vibration of –CH in methylene (–CH$_2$) and methyl (–CH$_3$) groups.[48] The adsorption peaks at 1654.03–1655.36 cm^{-1} and 1542.76–1544.25 cm^{-1} were attributed to the stretching vibration of amide I and amide II in proteins, respectively.[49] The peak at 1452.38–1453.01 cm^{-1} originated from the stretching vibration of –CH in aliphatics, while the band at 1398.17–1403.90 cm^{-1} was assigned to the stretching vibration of C=O in the carboxyl group.[22,23] The peak at 1242.53–1251.27 cm^{-1} was associated with the stretching vibration of P=O and the band at 1038.06–1079.71 cm^{-1} was assigned to the stretching vibration of C–O–C in uronic acid.[22,23] Thereafter, these functional groups, such as hydroxyl, carboxyl, methyl, and aldehyde groups on cell wall or EPS that involved in the removal of cadmium by complexation with them.

Zhang *et al.*[23] also used FTIR and found the adsorption mechanism of Cd^{2+} by *Burkholderia cepacia* GYP1 was mainly

Table 2 Kinetic studies of Cd^{2+} biosorption by *Synechocystis* sp. PCC6803

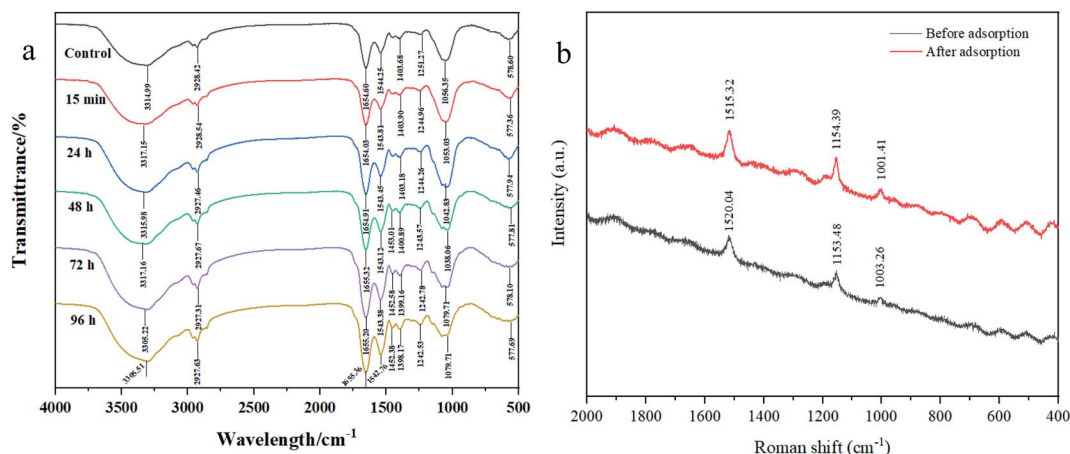| Adsorbent	Initial ion (mg L^{-1})	First order kinetic model			Second order kinetic model		
		q_e	K_1	R^2	q_e	K_2	R^2
Synechocystis sp. PCC6803	0.6	3.884	0.351	0.9977	4.066	0.190	0.9996
	1.0	7.660	0.269	0.9973	8.213	0.058	0.9989
	2.0	16.950	0.362	0.9970	17.712	0.046	0.9995

Fig. 6 FTIR (a) and Raman spectrum (b) analysis of *Synechocystis* sp. PCC6803 exposed to Cd^{2+}.

through complexation of functional groups with Cd^{2+}. It was also reported that hydroxyl, carbonyl, carboxyl, and amino groups in *Cupriavidus pauculus* 1490 that contributed a major role under the simulation of Cd(II), Ni(II), Cu(II) and Co(II).[50] Therefore, FTIR results demonstrated that these functional groups may participate in the Cd^{2+} adsorption process or play a major role in cyanobacteria resistance to heavy metals.

3.7.2 Raman spectrum analyses. Raman spectrum analysis was used to further identify structural information for *Synechocystis* sp. PCC6803 before and after Cd^{2+} adsorption. The Raman spectra (400–2000 cm^{-1}) before and after Cd^{2+} adsorption are shown in Fig. 6b. Three Raman peaks were observed before and after Cd^{2+} adsorption, located at 1515.32–1520.04, 1153.48–1154.39, and 1001.41–1003.26 cm^{-1}, respectively. These three peaks can be assigned to C=C, C–C, and phenylalanine.[51,52] In addition, the peak intensities after adsorption were significantly higher than those of the control. This indicated that C=C, C–C, and amino acid side chain (phenylalanine) exerted a prominent function in the Cd^{2+} adsorption process. Similar results were found in *Synechococcus* PCC7002, Yu *et al.*[53] found the C–C stretching and $C–H_2$ deformation after Cs(I) adsorption by Raman spectrum.

3.7.3 XPS analyses. To further investigate the adsorption mechanism of Cd^{2+} by *Synechocystis* sp. PCC6803, elemental composition changes before and after Cd^{2+} adsorption on cyanobacteria were analyzed by XPS (Fig. 7), the binding energy and atomic (%) are summarized in Table S4.† From the survey spectrum and high-resolution Cd 3d spectrum (Fig. 7a and b), Cd^{2+} was detected after adsorption, suggesting that Cd^{2+} was absorbed on the adsorbent surface. From the high-resolution C 1s spectrum (Fig. 7c and d), peaks at 283.15, 284.65, and 286.22 eV were observed, which corresponded to C–C, C–O, and C=O.[54] After adsorption, the atomic content of C–C increased from 62.63% to 66.94%, and C–O (18.01%) and C=O (19.34%) decreased to 15.90% and 17.16%, respectively. Fig. 7e and f show the high-resolution O 1s spectrum. Three peaks detected (529.51, 530.23, and 531.04 eV) were assigned to C=O, C–OH, and C–O.[54,55] After adsorption, the atomic content of C=O decreased from 37.76% to 29.53%, and C–OH (39.82%) and C–O (22.42%)

increased to 41.41% and 29.06%, respectively. The high-resolution N 1s spectrum (Fig. 7g and h) could be divided into two peaks including –NH (398.23 eV) and $–NH_2$ (398.35 eV),[56,57] and the atomic content of –NH increased from 75.68% to 86.68%, while $–NH_2$ decreased from 24.32% to 13.32% after adsorption. Thus the positions and atomic contents of these functional groups that transformed after Cd^{2+} adsorption, may be attributed to the complexation between metal ions and functional groups.

The results were consistent with previous reports, Xie *et al.*[22] used XPS and found that oxygen atom in protein carboxyl C–O might be the key site responsible for the EPS–Cd(II) complexation in *Chlorella vulgaris*. Based on XPS spectra analysis, Song *et al.*[57] also reported that the high adsorbability of *Aspergillus niger* was greatly due to a large number of nitrogen- and oxygen-containing functional groups on the surface of mycelia, which can easily form complexes with Co(II) and Eu(III). Thus XPS results in this research indicated that C–C, C–O, C=O, C–OH, –NH, and $–NH_2$ contributed major sites responsible for heavy metal adsorption.

3.8 SEM and TEM-EDX analyses

The surface morphology of cyanobacteria before and after Cd^{2+} adsorption was observed using SEM (Fig. 8A). Before Cd^{2+} adsorption, the cells exhibited integrated spherical structures, surface smoothness, and have specific dimensions. After adsorption, the surfaces of the cells were rough with some attachments aggregated on the surface. This could be due to Cd^{2+} aggregation around the cell surface and linked to the functional groups of EPS secreted by cyanobacteria cells, which was consistent with the results of a previous study. Ghoneim *et al.*[46] studied the surface morphology of *Ulva lactuca* before and after Cd^{2+} adsorption by SEM and found that Cd^{2+} precipitated around the cell surface. In this study, EDX analysis confirmed that Cd^{2+} accumulated on the cell surface.

TEM was mainly conducted to observe the spatial location of heavy metals adsorbed on the surface or interior of the cells. Significant changes were observed after Cd^{2+} adsorption, as
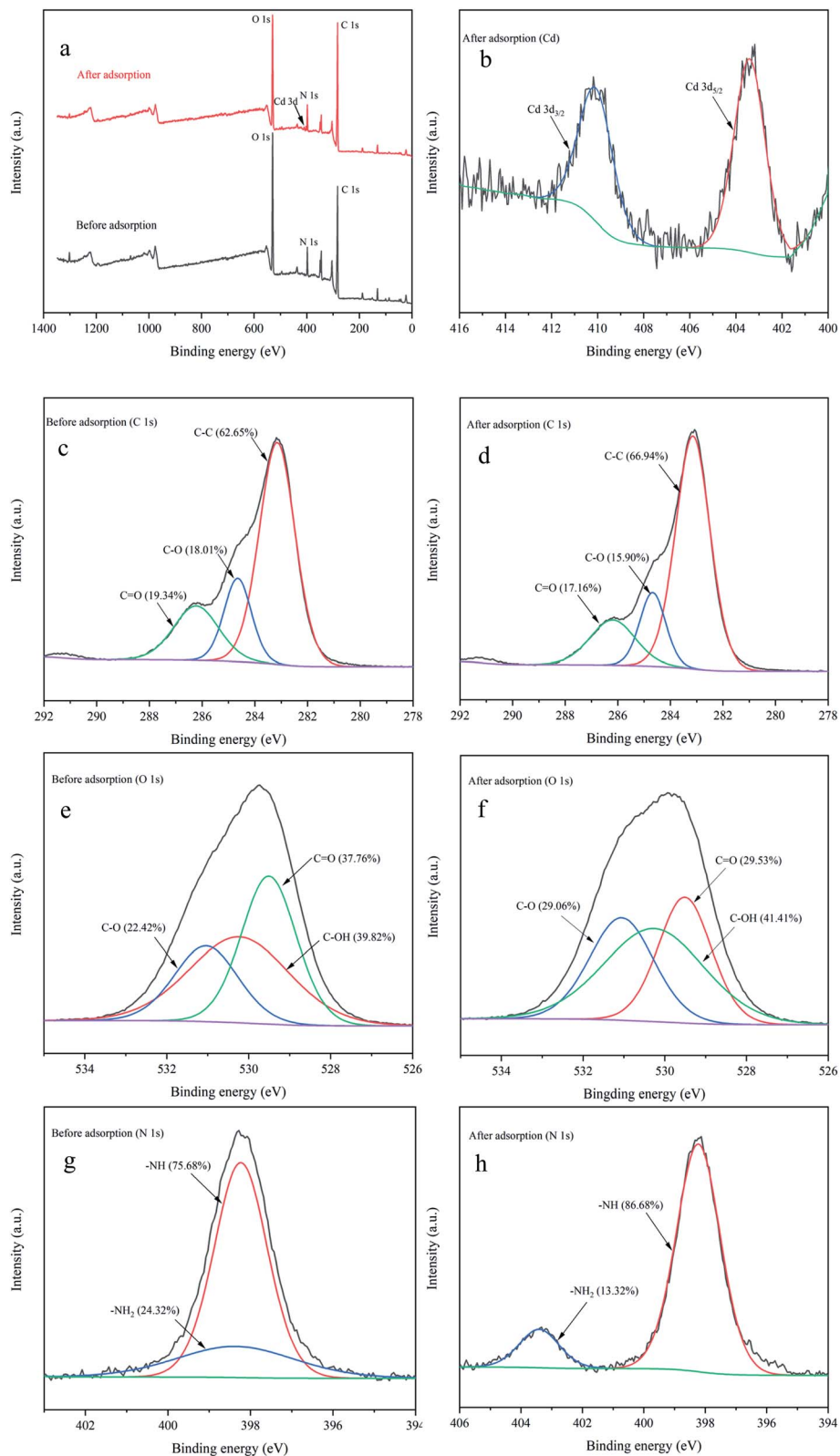
Fig. 7 XPS analysis before and after Cd^{2+} adsorption. survey spectrum (a); high-resolution spectra of Cd 3d (b); high-resolution spectra of C 1s before (c) and after (d) adsorption; high-resolution spectra of O 1s before (e) and after (f) adsorption; high-resolution spectra of N 1s before (g) and after (h) adsorption.

shown in Fig. 8B. The cell walls of cyanobacteria in the control group were smooth and complete, and the cytoplasm was relatively uniform, while the cell walls under Cd^{2+} stress were irregular and the various positions, sizes, and shapes of the metal particle aggregations were observed both the cell surface and intracellularly, indicating that Cd^{2+} could cross the
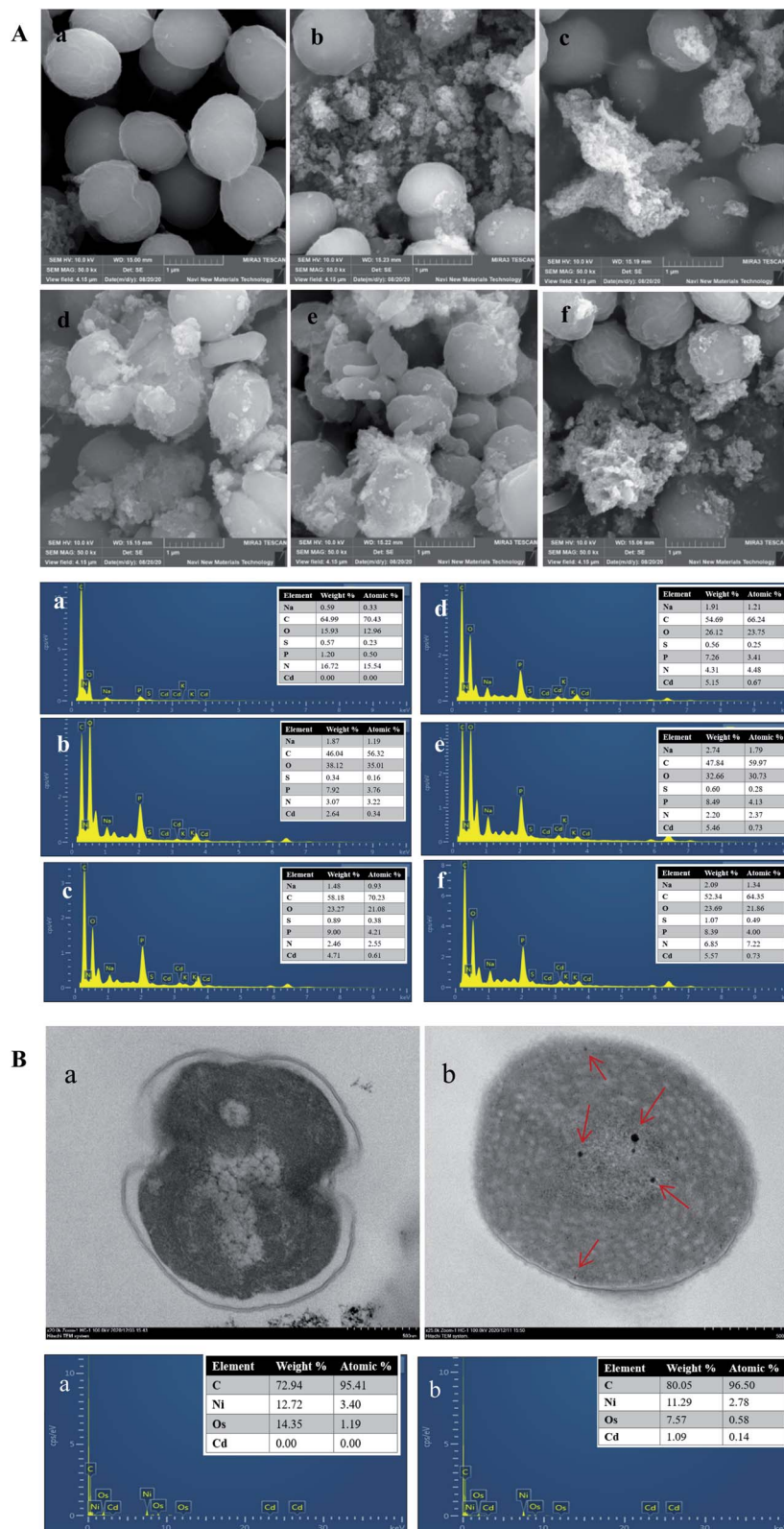
Fig. 8 SEM-EDX analysis (A) of *Synechocystis* sp. PCC6803 exposed to Cd^{2+} for 0 h (a), 15 min (b), 24 h (c), 48 h (d), 72 h (e) and 96 h (f). TEM-EDX analysis (B) of *Synechocystis* sp. PCC6803 before (a) and after (b) Cd^{2+} adsorption.

membrane by other mechanisms and was not merely fixed on the cell surface, which was similar to the results of previous studies.[19,23] Therefore, it is possible that two mechanisms existed in the Cd^{2+} adsorption process. Cd^{2+} was rapidly adsorbed on the cell surface by EPS and prevented it from entering the cells. In addition, Cd^{2+} may enter the cytoplasm
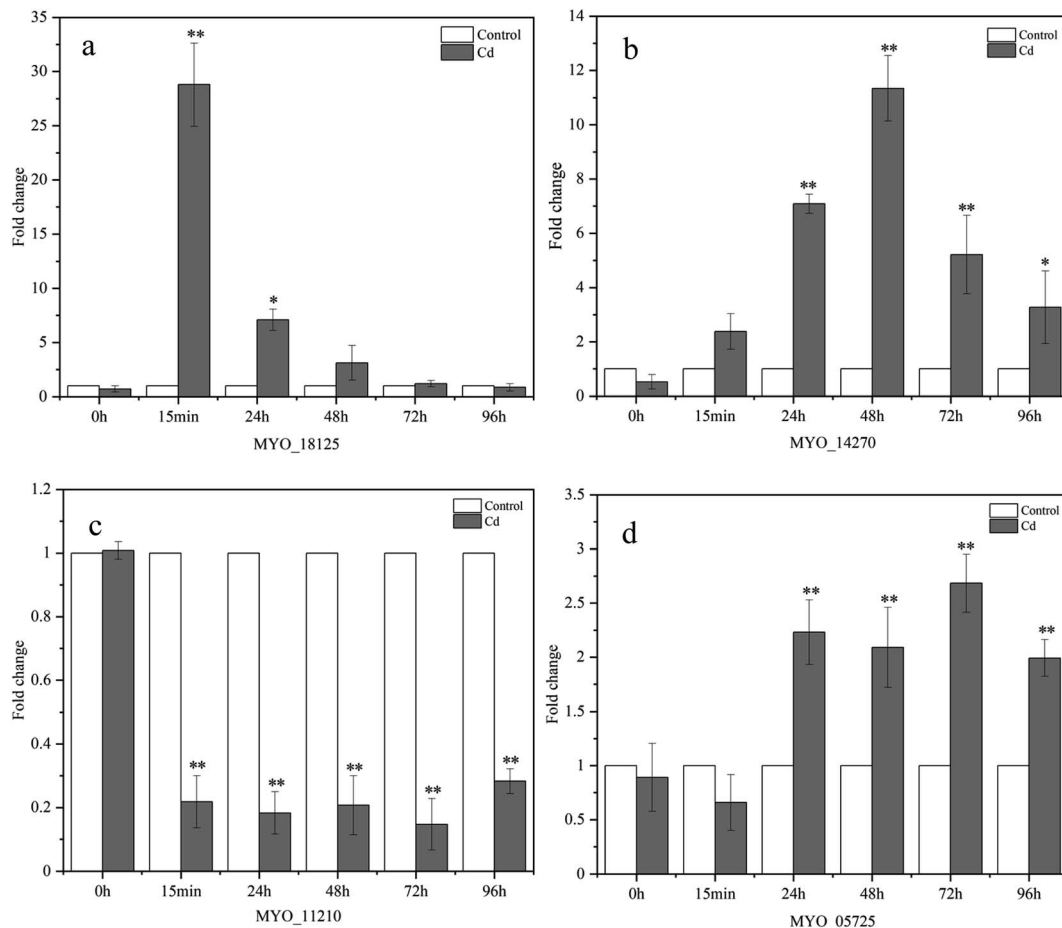
Fig. 9 Expression levels of Cd^{2+} adsorption (MYO_18125 (a), MYO_14270 (b), MYO_11210 (c)) and exopolysaccharide synthesis (MYO_05725 (d)) in *Synechocystis* sp. PCC6803 under Cd^{2+} stress, the relative expression level for each gene in control was set at 1. Asterisks indicate significant differences (*correlation is significant at the 0.05 level; **correlation is significant at the 0.01 level) from the control.

through the cytomembrane by transport systems. The EDX energy spectrum showed that Cd^{2+} entered the intracellular region.

3.9   The expression of genes involved in Cd^{2+} adsorption

In this research, RT-qPCR was performed to further investigate the expression profiles of genes involved in Cd^{2+} adsorption at the genetic level. The expression levels of these four genes are shown in Fig. 9. The expression of the MYO_18125 gene was up-regulated by 27.779, 6.098, 2.112, and 0.189 times at 15 min, 24, 48, and 72 h, respectively, and the most significant increase occurred at 15 min compared with the control. MYO_18125 gene encodes the CzcA family heavy metal efflux RND transporter, the high expression of the gene is possibly because of transporting Cd^{2+} to extracellular space to reduce toxicity.[58] The MYO_14270 gene was up-regulated separately by 1.379, 6.086, 10.342, 4.218, and 2.275 times at five time points, and the most significant up-regulation appeared at 48 h compared to the control. MYO_14270 gene encodes cadmium-translocating P-type ATPase (CadA), which could prevent Cd^{2+} from re-entering the cells once metal efflux is complete, and high expression of this gene may be in response to its detoxification

of Cd^{2+}. Furthermore, the gene expression levels of MYO_18125 and MYO_14270 increased initially and then decreased, up-regulation may be because the sites on the adsorbent's surface were sufficient and the Cd^{2+} concentration was high. The decrease in expression levels may be attributed to the low free Cd^{2+} concentration in the medium, heavy metal stress became weaker, and saturation of adsorption sites. In addition, The up-regulation of MYO_18125 gene was faster than that of MYO_14270 gene, and the maximum up-regulation multiple of MYO_18125 gene was 2.686-fold that of MYO_14270 gene, it was speculated that CzcA efflux system might play a major role in metal detoxification in *Synechocystis* sp. PCC6803. Nongkhlaw *et al.*[59] found that CzcA expression in *Chryseobacterium* sp. PMSZPI was 2-fold higher compared to CadA expression after 0.5 mM Cd^{2+} stress for 3 h, indicating that CzcA efflux system might play a major role in Cd^{2+} tolerance. The MYO_11210 gene encodes TrkA potassium uptake protein and the expression of the MYO_11210 gene was down-regulated at all time points, which was contrary to the previous studies, Chi *et al.*[12] found that the expression of the TrkA gene after cadmium adsorption was up-regulated compared to that of the control in *Bacillus paranthracis* NT1. In this study, down-regulation can be

speculated that the presence of Cd^{2+} may have inhibited potassium uptake protein activity. The expression of the MYO_05725 gene was up-regulated separately by 1.232, 1.091, 1.684, and 0.993 times at 24, 48, 72, and 96 h compared to the control, and the most significant increase occurred at 72 h. The MYO_05725 gene encodes the exopolysaccharide synthesis protein. The results of the gene expression levels were consistent with those of the content changes of exopolysaccharides. The high expression of this gene was probably because cyanobacteria secreted more exopolysaccharides to absorb heavy metals.

The results of RT-qPCR reflected that MYO_18125, MYO_14270, and MYO_05725 gene may participate in the regulation process of heavy metal adsorption, which preliminarily revealed the molecular regulation mechanism of *Synechocystis* sp. PCC6803 in response to Cd^{2+} adsorption. While the adsorption mechanism of heavy metals by cyanobacteria is a complex process, it may be regulated by a series of genes involved in growth and metabolism, heavy metal resistance, and transmembrane transport. Therefore, there are still many genes involved in Cd^{2+} adsorption that need to further identify. In addition, based on the results of RT-qPCR, genetic engineering technology can be applied to the treatment of heavy metals by cyanobacteria. Constructing mutants by silencing or over-expressing some genes related to Cd^{2+} adsorption and resistance, thus improving the adsorption efficiency of cyanobacteria to heavy metals.

4. Conclusion

In this study, *Synechocystis* sp. PCC6803 was used to evaluate the Cd^{2+} biosorption behavior and mechanism. The adsorption process was affected by many factors, including pH, temperature, initial Cd^{2+} concentration, and contact time. The adsorption process was fast and followed the pseudo-second order kinetic model, mainly based on chemical adsorption. The functional groups complexed with Cd^{2+} were mainly hydroxyl, amino, carbonyl, and carboxyl groups. GSH played an important role in alleviating Cd^{2+} toxicity as a component of the antioxidant system. In addition, EPS produced by *Synechocystis* sp. PCC6803 had significant impacts on Cd^{2+} adsorption by combining with heavy metals. SEM and TEM confirmed that Cd^{2+} can enter the cell, not only enriched on the cell surface. Moreover, RT-qPCR revealed the potential molecular regulatory mechanisms of *Synechocystis* sp. PCC6803 in the Cd^{2+} biosorption process. These results could provide a foundation for further investigation of the adsorption mechanism of heavy metals by other strains and provide theoretical guidance for the development of late-model biosorbents.

Conflicts of interest

The authors declare no actual or potential conflict of interest.

Acknowledgements

References

1 W. Huang and Z. M. Liu, *Colloids Surf., B*, 2013, **105**, 113–119.

2 T. Jiao, X. H. Chu, Z. Q. Gao, T. T. Yang, Y. Liu, L. Yang, D. Z. Zhang, J. L. Wang, B. P. Tang, K. Wu, Q. N. Liu and L. S. Dai, *Ecotoxicol. Environ. Saf.*, 2019, **182**, 109388.

3 Z. Xu, M. Dong, X. Peng, W. Ku, Y. Zhao and G. Yang, *Ecotoxicol. Environ. Saf.*, 2019, **171**, 301–312.

4 I. Vishan, B. Saha, S. Sivaprakasam and A. Kalamdhad, *Environ. Technol. Innovation*, 2019, **14**, 100323.

5 Y. K. Leong and J. S. Chang, *Bioresour. Technol.*, 2020, **303**, 122886.

6 J. He and J. P. Chen, *Bioresour. Technol.*, 2014, **160**, 67–78.

7 M. Jena, D. Pradhan and T. Das, *Int. J. Environ. Waste Manage.*, 2012, **9**, 221–231.

8 E. N. Bakatula, E. M. Cukrowska, I. M. Weiersbye, L. Mihaly-Cozmuta, A. Peter and H. Tutu, *J. Geochem. Explor.*, 2014, **144**, 492–503.

9 D. Zhang, X. Pan, K. M. Mostofa, X. Chen, G. Mu, F. Wu, J. Liu, W. Song, J. Yang, Y. Liu and Q. Fu, *J. Hazard. Mater.*, 2010, **175**, 359–365.

10 J. N. Nkoh, R. K. Xu, J. Yan, J. Jiang, J. Y. Li and M. A. Kamran, *Environ. Pollut.*, 2019, **247**, 136–145.

11 Y. Zhang, X. Wang, T. Shan, S. Pang and N. Xu, *Marine Genomics*, 2019, **47**, 100671.

12 Y. Chi, Y. Huang, J. Wang, X. Chen, S. Chu, K. Hayat, Z. Xu, H. Xu, P. Zhou and D. Zhang, *Sci. Total Environ.*, 2020, **741**, 140422.

13 S. Naveed, Q. Yu, C. Zhang and Y. Ge, *Environ. Pollut.*, 2020, **261**, 114233.

14 L. Shen, Z. Li, J. Wang, A. Liu, Z. Li, R. Yu, X. Wu, Y. Liu, J. Li and W. Zeng, *Environ. Sci. Pollut. Res.*, 2018, **25**, 20713–20722.

15 S. Ozturk, B. Aslim, Z. Suludere and S. Tan, *Carbohydr. Polym.*, 2014, **101**, 265–271.

16 H. Xu, H. Cai, G. Yu and H. Jiang, *Water Res.*, 2013, **47**, 2005–2014.

17 L. Zhu, J. Zhou, M. Lv, H. Yu, H. Zhao and X. Xu, *Chemosphere*, 2015, **121**, 26–32.

18 X. Pan, J. Liu and D. Zhang, *Colloids Surf., B*, 2010, **80**, 103–106.

19 T. Lan, Y. Feng, J. Liao, X. Li, C. Ding, D. Zhang, J. Yang, J. Zeng, Y. Yang, J. Tang and N. Liu, *J. Environ. Radioact.*, 2014, **134**, 6–13.

20 L. Fang, C. Zhou, P. Cai, W. Chen, X. Rong, K. Dai, W. Liang, J. D. Gu and Q. Huang, *J. Hazard. Mater.*, 2011, **190**, 810–815.

21 Y. G. Bermúdez, I. L. R. Rico, O. G. Bermúdez and E. Guibal, *Chem. Eng. J.*, 2011, **166**, 122–131.

22 Q. Xie, N. Liu, D. Lin, R. Qu, Q. Zhou and F. Ge, *Environ. Pollut.*, 2020, **263**, 114102.

23 J. Zhang, Q. Li, Y. Zeng, J. Zhang, G. Lu, Z. Dang and C. Guo, *Ecotoxicol. Environ. Saf.*, 2019, **176**, 162–169.

24 W. Shi, G. Zhang, F. Li, J. Feng and X. Chen, *Sci. Total Environ.*, 2020, **742**, 140606.

25 T. D. Schmittgen and K. J. Livak, *Nat. Protoc.*, 2008, **3**, 1101–1108.

26 C. General, *OECD Guidelines for the Testing of Chemicals*, 2006, **1**, 1.

27 Q. L. Zhu, S. N. Guo, F. Wen, X. L. Zhang, C. C. Wang, L. F. Si, J. L. Zheng and J. Liu, *Aquat. Toxicol.*, 2019, **207**, 153–162.

28 H. X. Li, Y. Xiao, L. L. Cao, X. Yan, C. Li, H. Y. Shi, J. W. Wang and Y. H. Ye, *PLoS One*, 2013, **8**, e73380.

29 D. Laporte, N. Valdes, A. Gonzalez, C. A. Saez, A. Zuniga, A. Navarrete, C. Meneses and A. Moenne, *Aquat. Toxicol.*, 2016, **177**, 433–440.

30 C. S. Seth, P. Kumar Chaturvedi and V. Misra, *Ecotoxicol. Environ. Saf.*, 2008, **71**, 76–85.

31 Z. Teng, W. Shao, K. Zhang, Y. Huo, J. Zhu and M. Li, *Chem. Eng. J.*, 2019, **375**, 122113.

32 B. Ma, Z. Li, S. Wang, Z. Liu, S. Li, Z. She, N. Yu, C. Zhao, C. Jin, Y. Zhao, L. Guo and M. Gao, *Environ. Pollut.*, 2019, **251**, 81–89.

33 N. Li, D. Wei, S. Wang, L. Hu, W. Xu, B. Du and Q. Wei, *J. Colloid Interface Sci.*, 2017, **490**, 754–761.

34 J. Hou, Y. Yang, P. Wang, C. Wang, L. Miao, X. Wang, B. Lv, G. You and Z. Liu, *Environ. Sci. Pollut. Res.*, 2017, **24**, 226–235.

35 G. P. Sheng and H. Q. Yu, *Water Res.*, 2006, **40**, 1233–1239.

36 W. Chen, P. Westerhoff, J. A. Leenheer and K. Booksh, *Environ. Sci. Technol.*, 2003, **37**, 5701–5710.

37 X. Pan, J. Liu, W. Song and D. Zhang, *Front. Environ. Sci. Eng.*, 2012, **6**, 493–497.

38 L. Zhu, H. Y. Qi, M. L. Lv, Y. Kong, Y. W. Yu and X. Y. Xu, *Bioresour. Technol.*, 2012, **124**, 455–459.

39 M. Alyassin, G. M. Campbell, H. Masey O'Neill and M. R. Bedford, *Food Chem.*, 2020, **315**, 126221.

40 F. Çolak, N. Atar, D. Yazıcıoğlu and A. Olgun, *Chem. Eng. J.*, 2011, **173**, 422–428.

41 M. Aryal and M. Liakopoulou-Kyriakides, *Environ. Monit. Assess.*, 2015, **187**, 4173.

42 S. E. Oh, S. H. A. Hassan and J. H. Joo, *World J. Microbiol. Biotechnol.*, 2009, **25**, 1771–1778.

43 X. Ma, W. Cui, L. Yang, Y. Yang, H. Chen and K. Wang, *Bioresour. Technol.*, 2015, **185**, 70–78.

44 J. Bai, X. Yang, R. Du, Y. Chen, S. Wang and R. Qiu, *J. Environ. Sci.*, 2014, **26**, 2056–2064.

45 X. Li, D. Li, Z. Yan and Y. Ao, *RSC Adv.*, 2018, **8**, 30902–30911.

46 M. M. Ghoneim, H. S. El-Desoky, K. M. El-Moselhy, A. Amer, E. H. Abou El-Naga, L. I. Mohamedein and A. E. Al-Prol, *Egypt. J. Aquat. Res.*, 2014, **40**, 235–242.

47 P. B. Vilela, C. A. Matias, A. Dalalibera, V. A. Becegato and A. T. Paulino, *J. Environ. Chem. Eng.*, 2019, **7**, 103327.

48 P. M. Thabede, N. D. Shooto, T. Xaba and E. B. Naidoo, *J. Environ. Chem. Eng.*, 2020, **8**, 104045.

49 Z. Zhang, K. Yan, L. Zhang, Q. Wang, R. Guo, Z. Yan and J. Chen, *J. Hazard. Mater.*, 2019, **374**, 420–427.

50 W. Zeng, S. Zhang, M. Xia, X. Wu, G. Qiu and L. Shen, *RSC Adv.*, 2020, **10**, 20385–20394.

51 C. E. E. Grace, P. K. Lakshmi, S. Meenakshi, S. Vaidyanathan, S. Srisudha and M. B. Mary, *Spectrochim. Acta, Part A*, 2020, **224**, 117382.

52 M. Tang, G. D. McEwen, Y. Wu, C. D. Miller and A. Zhou, *Anal. Bioanal. Chem.*, 2013, **405**, 1577–1591.

53 R. Yu, H. Chai, Z. Yu, X. Wu, Y. Liu, L. Shen, J. Li, J. Ye, D. Liu, T. Ma, F. Gao and W. Zeng, *Microorganisms*, 2020, **8**, 491.

54 X. Xie, X. Zhao, X. Luo, T. Su, Y. Zhang, Z. Qin and H. Ji, *Chin. J. Chem. Eng.*, 2020, DOI: 10.1016/j.cjche.2020.06.003.

55 J. J. Ojeda, M. E. Romero-González, R. T. Bachmann, R. G. Edyvean and S. A. Banwart, *Langmuir*, 2008, **24**, 4032–4040.

56 S. J. Yuan, M. Sun, G. P. Sheng, Y. Li, W. W. Li, R. S. Yao and H. Q. Yu, *Environ. Sci. Technol.*, 2011, **45**, 1152–1157.

57 W. Song, J. Liang, T. Wen, X. Wang, J. Hu, T. Hayat, A. Alsaedi and X. Wang, *Chem. Eng. J.*, 2016, **304**, 186–193.

58 X. Xia, S. Wu, Z. Zhou and G. Wang, *J. Hazard. Mater.*, 2021, **401**, 123685.

59 M. Nongkhlaw and S. R. Joshi, *PLoS One*, 2019, **14**, e0216995.